International Journal of Applied Mathematics and Computing Science. Volume 4, Issue 1, (2015) 10-20
http://www.cayley-nielson.com/ijamcs

A Numerical Simulation Method for IC Interconnect Structures Electro-migration Failure

Anderson Wisdom
School of Information, The University of Texas at Austin, Austin, TX 78173, USA
E-mail: AndersonW@utexas.edu

Abstract

Finite element method (FFM) is a very efficient approach for solving various mathematical problems. It has been extensively applied in the engineering. Electro-migration (EM) is a diffusion controlled mass transport process in IC interconnects structure. This paper investigates the electro-migration induced void and hillock generation in interconnect structures and presents a new algorithm for electro-migration failure analysis using finite element method. The methodology is developed based on discretized weighted residual method in a user-defined finite element analysis framework to solve the local governing equation with the variable of atomic density. The new method takes the advantage of solving the variable of atomic density, it avoids directly solving the divergences of the atomic flux, which includes the atomic density gradient items and is very hard and challenging to get the solution by traditional method. The comparison of void/hillock formation and the time to failure (TTF) life through numerical example of the standard wafer level electro-migration accelerated test (SWEAT) structure with the measurement results are studied and discussed.

Keywords: electro-migration; interconnect; finite element analysis; weighted residual method.

1. Introduction

Electro-migration is a phenomenon of mass transport in metallization structures when the metallization is stressed with high electrical current density. With further dimensional scaling down of very-large-scale integration (VLSI) circuits and increasing of current density, electro-migration in IC interconnects continues to be a subject of concern. Under high current density, mass accumulation on the anode side, causes local compression and eventually the mass is squeezed out of the surface to form protrusions which are called hillocks and whiskers. When the protrusions contact with a circuit nearby, it causes short circuit failure. While on the cathode side, mass depletion causes tension and vacancy accumulation. Voids nucleating under tensile stress will grow and coalesce until a void forms which leads to an electrical failure [1].

In classical electro-migration studies, Black developed an empirical equation to relate the median time to failure with respect to the current density and temperature of the metal interconnects, and has been widely used in industry till now [2]. But a lot of experimental work and modeling have shown that the Black's theory is not enough accurate to evaluate the reliability [3-4]. This is because Black's equation considers the electron wind force as the sole driving force responsible for the EM failure. In recent years, there are a lot of efforts attempting to predict the electro-migration failure through modeling. Dalleau et al developed the finite element model for prediction of electro-migration voids in interconnects, which considers three mechanisms including the electro-migration, the thermo-migration and the stress-migration [5]. Later, Basaran and Lin [6] developed the damage mechanics for EM in interconnect, which is

ISSN 2333-2425 / Copyright © 2015 CAYLEY NIELSON PRESS, INC.
March, 2015

governed by the vacancy conservation equation and is equivalent to mass conservation equation. There are many other researchers also studied the atomic flux divergence (AFD) method based on finite element models [7-9]. However, most of the studies were focus on the electro-migration induced voids and few publications have been seen for the investigation of the hillock. In addition, the accuracy of the AFD prediction method is always an issue. Tan et al found that the conventional atomic flux divergence formulation is not accurate in the predicting void nucleation site in a very thin film structure [8].

In fact, due to the coupled metaphysics characteristic of EM, it is extremely difficult to predict the exact location of EM induced void/hillock nucleation and to simulate the subsequent void/hillock evolution in an arbitrary interconnect segment. Therefore, it is necessary to integrate the knowledge obtained from the research on this specific mechanism and to develop a practical and general numerical method for predicting the EM void and hillock damage.

This paper investigates the electro-migration induced void and hillock generation in a wafer level interconnects structure. The methodology is developed based on discretized weighted residual method (WRM) in a user-defined finite element analysis (FEA) framework to solve the local EM mass continuity equation with the variable of atomic density. The local iteration procedure of the EM governing equation for the atomic concentration redistribution and its time step scheme are developed and discussed. Finally, a numerical example of SWEAT structure is studied, and the comparison with the measurement results is discussed.

2. Basic equations for electro-migration

Electro-migration is a diffusion controlled mass transport process in a interconnect structure. The time dependent evolution equation of the local atomic density caused by an applied current is the mass balance (continuity) equation,

$$\nabla \cdot \mathbf{q} + \frac{\partial c}{\partial t} = 0 \tag{1}$$

where c is the normalized atomic density (NAD), $c=C/C_0$, C is the actual atomic density and C_0 is the initial (equilibrium state) atomic density in the absence of a stress field, t is the time; $\mathbf{q}$ is the total normalized atomic flux.

The driving forces of atomic flux may include electron wind, temperature gradients, hydrostatic stress gradients and atomic density gradient, thus,

$$\mathbf{q} = \mathbf{q}_{Ew} + \mathbf{q}_{Th} + \mathbf{q}_S + \mathbf{q}_C \tag{2}$$

where

Electron wind term: $$\mathbf{q}_{Ew} = \frac{Dc}{kT} Z^* e \rho \mathbf{j} \tag{2a}$$

Temperature gradients term: $$\mathbf{q}_{Th} = -\frac{Dc}{kT} Q^* \frac{\nabla T}{T} \tag{2b}$$

Stress gradients term: $$\mathbf{q}_S = \frac{Dc}{kT} \Omega \nabla \sigma_m \tag{2c}$$

Atomic density gradient term: $$\mathbf{q}_C = -D \nabla c \tag{2d}$$

In the above, k is Boltzmann's constant; e is the electronic charge; Z^* is the effective charge which is determined experimentally; T is the absolute temperature; ρ is the resistivity which is calculated as $\rho = \rho_0 (1 + \alpha (T - T_0))$, where is the temperature coefficient of the metallic material, ρ_0 is the resistivity at T_0; $\mathbf{j}$ is the current density vector; Q^* is the heat of transport; Ω is the atomic volume; $\sigma_m = (\sigma_1 + \sigma_2 + \sigma_3)/3$ is the local hydrostatic stress, where $_1$, $_2$, $_3$ are the components of principal

stress; D is the effective atom diffusivity, $D = D_0 \exp(-E_a / kT)$, where E_a is the activation energy, D_0 is the effective thermally activated diffusion coefficient.

Substituting Eqs. (2a-2d) into Eq. (2), it yields

$$\mathbf{q} = c \cdot \mathbf{F}(T, \sigma_m, \mathbf{j}, \cdots) - D\nabla c \tag{3}$$

where

$$\mathbf{F}(T, \sigma_m, \mathbf{j}, \cdots) = \frac{D}{kT} Z^* e\rho \mathbf{j} - \frac{D}{kT} Q^* \frac{\nabla T}{T} + \frac{D}{kT} \Omega \nabla \sigma_m \tag{4}$$

For the EM evolution equation (Eq. (1)) on any enclosed domain V with the corresponding boundary Γ, the atomic flux boundary conditions of a metal interconnects can be expressed as

$$\mathbf{q} \cdot \mathbf{n} = q_0 \quad \text{on} \quad \Gamma \tag{5}$$

For blocking boundary condition,

$$q_0 = 0 \quad \text{on} \quad \Gamma \tag{6}$$

At the initial time, the normalized atomic density is assumed to be

$$c_0 = 1 \tag{7}$$

The above equations and boundary conditions constitute the boundary value problem that governs the atomic transport during EM. This boundary value problem must be solved accurately in order to adequately describe the continuous atom redistribution and to capture the realistic kinetics of void nucleation and growth as a function of the interconnect architecture, segment geometry, material properties, and stress conditions.

3. Electro-migration evolution algorithm

3.1. Atomic density redistribution algorithm

Eq. (1) describes the atom density evolution at any point of the considered segment characterized by the given current density $\mathbf{j}$, T, gradients of temperature and stress. Thus, to obtain a complete solution of the problem we should determine in coupled manner the evolution of the current, temperature, and stress distributions in the considered segment, caused by continuous atom density redistribution. Assuming that an almost immediate establishment of a new equilibrium in the current, temperature, and stress distributions accompanies slow atom migration, we can employ the steady-state solutions for current, temperature, and stress, obtained for the different atom density distributions. After we obtain the current, temperature, stress and atomic density distribution in an incremental step, the atomic density redistribution need to be solved based on Eq. (1) in the next step.

In the finite element method, we seek an approximation solution for Eq. (1) to develop a new local simulation algorithm for the local atomic density in a wafer level interconnect device. The first step is to multiply the time dependent EM evolution equation with a weighted residual function w and integrate over the enclosed domain V based on the vector identity by applying the Gauss-Ostrogradsky divergence theorem to the product of the scalar function w and the atomic flux vector field:

$$\int_V w(\nabla \cdot \mathbf{q} + \dot{c}) \mathrm{d}V = \int_V w\dot{c} \mathrm{d}V + \int_V w \cdot (\nabla \cdot \mathbf{q}) \mathrm{d}V = \int_V w\dot{c} \mathrm{d}V - \int_V \frac{\partial w}{\partial \mathbf{n}} \cdot \mathbf{q} \mathrm{d}V + \int_\Gamma w \cdot (\mathbf{q} \cdot \mathbf{n}) \mathrm{d}\Gamma = 0 \tag{8}$$

From Eq. (8) with considering the atomic flux boundary condition of Eq. (5),

$$\int_V w\dot{c} dV - \int_V \frac{\partial w}{\partial \mathbf{n}} \cdot \mathbf{q} dV = -\int_\Gamma w q_0 d\Gamma \tag{9}$$

Next, assume that $c = \sum_{j=1}^{n} \psi_j c^j$, $\dot{c} = \sum_{j=1}^{n} \psi_j \dot{c}^j$ and $w = \psi_i$ (for Galerkin Method), where ψ_i is the shape function of the element. After element discretization, the matrix form of Eq. (9) can be written as

$$[\mathbf{M}]\{\dot{c}\}+[\mathbf{K}]\{c\}=\{\mathbf{Y}\} \tag{10}$$

where the mass matrix $[\mathbf{M}]$ is independent of time, the stiffness matrix $[\mathbf{K}]$ will remain constant in an incremental step where we consider the current density $\mathbf{j}$ and the local hydrostatic stress σ_m is also a constant in the present incremental step, $\{\mathbf{Y}\}$ is the known term.

For an element *e* with volume V_e, mass matrix $[\mathbf{M}]$ and stiffness matrix $[\mathbf{K}]$ can be discretized as

$$\begin{cases} [\mathbf{M}]_{ij}^{e}=\int_{V_e}\psi_i\psi_j dV_e \\ [\mathbf{K}]_{ij}^{e}=\int_{V_e}\left[-\left(\frac{\partial\psi_i}{\partial\mathbf{n}}\cdot\mathbf{F}\right)\psi_j+D\left(\frac{\partial\psi_i}{\partial x}\frac{\partial\psi_j}{\partial x}+\frac{\partial\psi_i}{\partial y}\frac{\partial\psi_j}{\partial y}+\frac{\partial\psi_i}{\partial z}\frac{\partial\psi_j}{\partial z}\right)\right]dV_e \end{cases} \tag{11}$$

where $[\mathbf{M}]_{ij}^{e}$ and $[\mathbf{K}]_{ij}^{e}$ are discretized forms of mass matrix $[\mathbf{M}]$ and stiffness matrix $\{\mathbf{K}\}$ respectively..

The most commonly used local iteration scheme for solving the above equation is the -family of approximation method in which a weighted average of the time derivatives at two consecutive time steps is approximated by linear interpolation of the values of the variable at two steps:

$$(1-\alpha)\dot{c}_{t_i}+\alpha\dot{c}_{t_{i+1}}=\frac{c_{t_{i+1}}-c_{t_i}}{\Delta t},\quad \text{for}\quad 0\le\alpha\le 1 \tag{12}$$

In this work, $\alpha=0.5$ is used. Such method is called the Crank-Nicolson scheme which is stable and has the accuracy order of $O((\ t)^2)$ [10].

It follows from Eq. (10) and Eq. (12) with considering the incremental step that

$$([\mathbf{M}]+\alpha\Delta t[\mathbf{K}])\{c_{t_{i+1}}\}=([\mathbf{M}]-(1-\alpha)\Delta t[\mathbf{K}])\{c_{t_i}\}+\{\overline{\mathbf{Y}}\}_{i,i+1} \tag{13}$$

where

$$\{\overline{\mathbf{Y}}\}_{i,i+1}=(1-\alpha)\Delta t\{\overline{\mathbf{Y}}\}_{t_i}+\alpha\Delta t[\mathbf{M}]\{\overline{\mathbf{Y}}\}_{t_{i+1}} \tag{14}$$

Thus, the normalized atomic density *c* in the $(i+1)^{\text{th}}$ step can be obtained based on Eq. (14) in terms of the corresponding value in the ith step. Since the initial atomic density $c_0=1$ is known, the above equations provide the solution to *c* at any time step. For the blocking boundary condition, $\{\overline{\mathbf{Y}}\}_{i,i+1}=\{0\}$.

3.2 Simulation algorithm of EM induced void and hillock evolution

The damage induced by electro-migration appears as voids and hillocks. Lifetime and failure location in an interconnect structure can be predicted by means of numerical simulation of the process of void/hillock incubation, initiation and growth. The changes in current density and temperature distribution due to void growth should be taken into account in simulation.

The computation procedure of EM induced void and hillock evolution based on atomic density redistribution algorithm is shown in Fig. 1. The calculation consists of an incubation period and a growth period for a void/hillock. In the simulation for the incubation period, at first, the initial distributions of current density and temperature in the interconnect structure are obtained by 3D finite element method analysis based on ANSYS. Then, atom density redistribution in the interconnect structure are solved based on the atom density redistribution algorithm using a user-defined FORTRAN code.

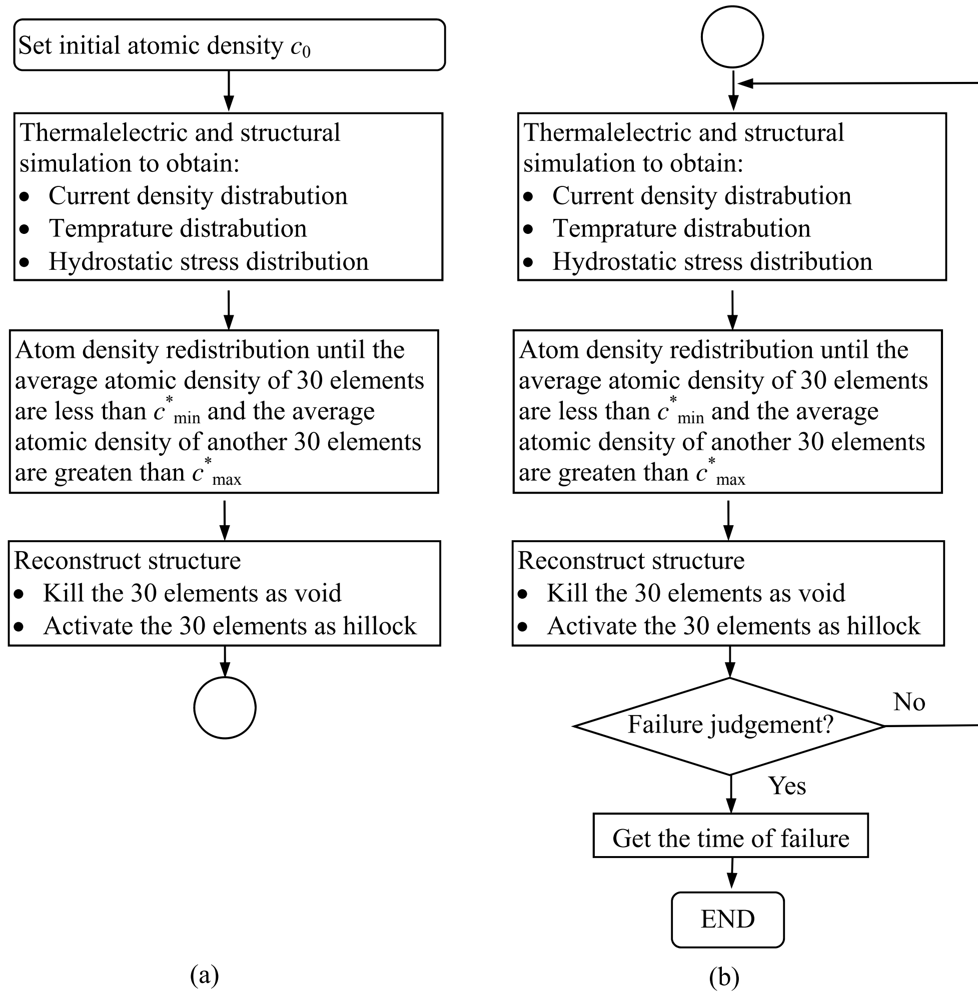

(a) Incubation period (b) Void/hillock growth period

Figure 1. Computational procedure for numerical simulation of the EM evolution

Assume that there is a critical atomic density for void initiation c^*_{min}, and for hillock initiation c^*_{max}. When c is less than or equal to c^*_{min} ($c \le c^*_{min}$), the void will appear or grow. Conversely, when c is greater than or equal to c^*_{max} ($c \ge c^*_{max}$), the hillock will be generated. On the other hand, when the average c values of all the elements is within c^*_{min} and c^*_{max} ($c^*_{max} \ge c \ge c^*_{min}$), which it is regarded as not having reached the critical atomic density. The values, c^*_{min} and c^*_{max} can be gotten from experiments. $c^*_{min} = 0.95$ and $c^*_{max} = 1.05$ of a thin film interconnect line was determined by Sasagawa and his coworkers [11]. In the simulation procedure of the void/hillock growth period, once the average atomic density value of the elements are less than the critical atomic density for void initiation c^*_{min}, the corresponding elements will be killed (“element death”) and once the average atomic density value of the

elements are greater than the critical atomic density for hillock initiation $c^*_{\max}$, the corresponding elements will be activated ("element alive"), seen as in Fig.2. To achieve the "element death" effect, ANSYS does not actually remove "killed" elements. Instead, it deactivates them by changing the element material attribute, such as to the elastic module with 1.0E-6 of the source elastic module, to the resistivity with 1.0E-6 of the source resistivity. This actually multiplies the stiffness by a severe reduction factor.

In semiconductor industry, the resistance excess 15% of initial value is the EM failure criterion of an interconnect structure, which also used in this work. This criterion is used in this work to get the final TTF. For high density circuits and interconnects layout, another failure criterion is defined for hillock, that is when the hillock size reaches the 70% width of the line. This criterion is intended to set to avoid the circuit short when the hillock appears.

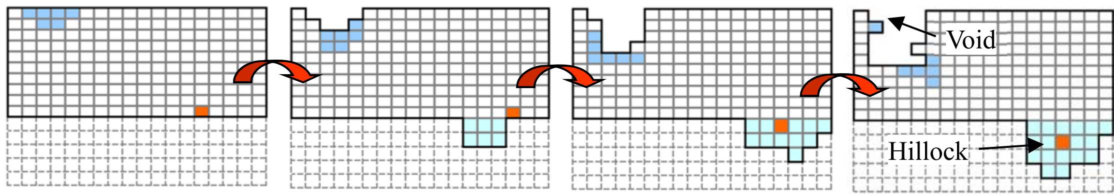

Figure 2. Schematic process flow of void and hillock evolution

3.3 Algorithm Validation

In order to verify the algorithm of atomic density redistribution, we consider one-dimension model of a metal wire in length l subjected to constant current as an example. In the electro-migration evolution equation, it only took into account the electronic wind and atomic density gradient caused by the atomic flux, that is

$$\mathbf{q} = \mathbf{q}_{Ew} + \mathbf{q}_c = \frac{Dc}{kT} Z^* e\rho \mathbf{j} - D\frac{\partial c}{\partial x} \tag{15}$$

where x is the coordinate value of electric field.

Consider the blocking boundary conditions:

$$\begin{cases} c(x,0) = 1, & x \in [0,l] \\ q(0,t) = 0, & \text{at anode} \\ q(l,t) = 0, & \text{at cathode} \end{cases} \tag{16}$$

where t is the time.

It can be solved as follows [12],

$$c(0,\tau) = \frac{p}{1-e^{-p}} - \sum_{k=1}^{\infty} \frac{32\pi^2 k^2 p\left\{1-(-1)^k e^{\frac{p}{2}}\right\}}{\left(p^2 + 4\pi^2 k^2\right)^2} e^{-\left(\frac{\pi^2 k^2}{p^2} + \frac{1}{4}\right)\tau} \tag{17}$$

where $\tau = \frac{p^2 Dt}{l^2}$ is the normalized time; $p = al$, $a = \frac{Z^* e\rho j}{kT}$, $1/a$ is considered as a characteristic length for electro-migration and is also called to be the "Blech length".

To verify the new algorithm for analysis of electro-migration, an aluminum wire with 7μm×7μm cross-section under 1E+12A/m^2 current density at 400K temperature is taken as an example as shown in Fig. 3. The blocking boundary conditions of Eq. (16) are considered. The analytical solutions of Eq. (17) can be solved by Matlab in which the former 100 series is taken in this paper.

Fig. 4 shows the normalized atomic density of anode at the different normalized time τ with the

different lengths of conductors, in which the x-coordinate takes the normalized time τ. As shown in Fig. 4, the normalized atomic density presented in this paper has a good agreement with the analytical solution. At the beginning, with the τ increases, the normalized atomic density also increases which will result in hillocks at anode. And then the normalized atomic density will reach a steady state (saturation normalized atomic density) as τ continues increasing. In addition, the presence of the saturation values denoted by the horizontal lines at long times indicates a length effect. As the normalized time $\tau \to \infty$, we can see that the normalized saturation atomic density increases with p.

$$c(0,\infty) = \frac{p}{1-e^{-p}} = \frac{pe^{p}}{e^{p}-1} \tag{18}$$

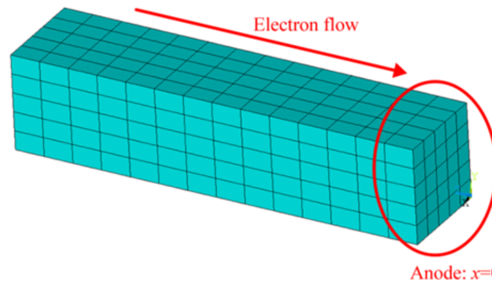

Figure 3. Mesh of Al wire model (p=2)

With p=2 (a line with twice the Blech length), for example, the different mesh densities of the model (similarly as Fig. 3) and different time increment (Δt) are considered for studying the impact of the mesh density and the time increment on the solution of atomic density based on the algorithm in this paper.

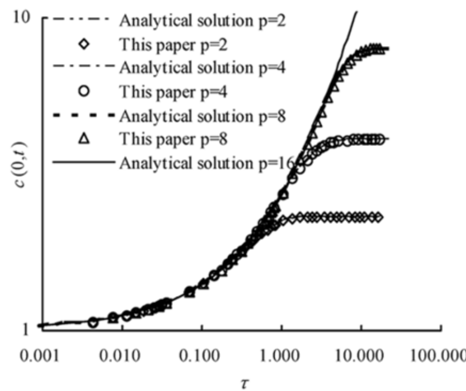

Figure 4. NAD at anode with different normalized time

Table 1. Saturation NAD at anode with different time increment under p=2

p=2	Saturation NAD			
Time increment: Δt	0.001	0.01	10	100
Number of elements: 350	2.3118	2.3118	2.3118	2.3118

Table 2. Saturation NAD at anode with different mesh densities under p=2

Number of elements	Saturation NAD, p=2		Error (%)
	Analytical solution	Result of this paper	

176	2.3230	2.3110	-0.0865%
350		2.3118	-0.0519%
882		2.3123	-0.0303%
2700		2.3127	-0.0130%

Table 1 shows the comparison of the saturation NAD at anode between analysis solution and that of this paper with different time increment under p=2 by using the model of 350 elements as Fig. 3. It can be seen from Table 1, the algorithm in this paper does not depend on the time increment, the algorithm is stable due to the implicit format used. Table 2 shows the comparison of the saturation NAD at anode between the analytical solutions and the results from this paper with different element densities and Δt=0.01 under p=2. It can be seen from Table 2, the algorithm in this paper is not dependent on the density of the mesh discretization.

4. Numerical example

Dalleau et al [13] have conducted the electro-migration test for a SWEAT structure. A 1.1μm silicon dioxide layer was thermally growth on the silicon substrate. The section of aluminum alloy (with 1% Si) metallization structure is 0.88μm×2μm. The length of the inner metal line is 10μm and the thickness of the silicon substrate is taken to be 5μm. For the hillock growth, some elements are built in advance around the aluminum line. These elements are killed in the beginning of simulation, and the corresponding elements will be activated when the average atomic density value of aluminum line elements are greater than c^*_{max}. Here due to symmetry, only a half of the structure was modeled. The three-dimensional finite element model for SWEAT structure is shown in Fig. 5. The related thermal mechanical, electrical and electro-migration parameters of SWEAT structure are taken from ref. [14].

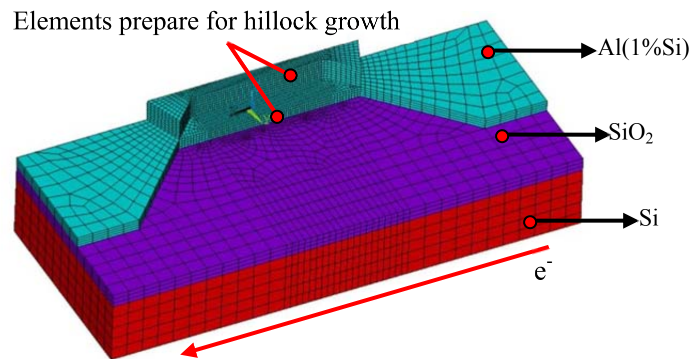

Figure 5. SWEAT structure and its mesh

The structure is considered to be stress-free at 400℃ (fabrication process temperature) for the simulations. In addition, a blocking boundary condition for diffusion is assumed, such that the diffusion flux is zero at each end as well as both sides of the line.

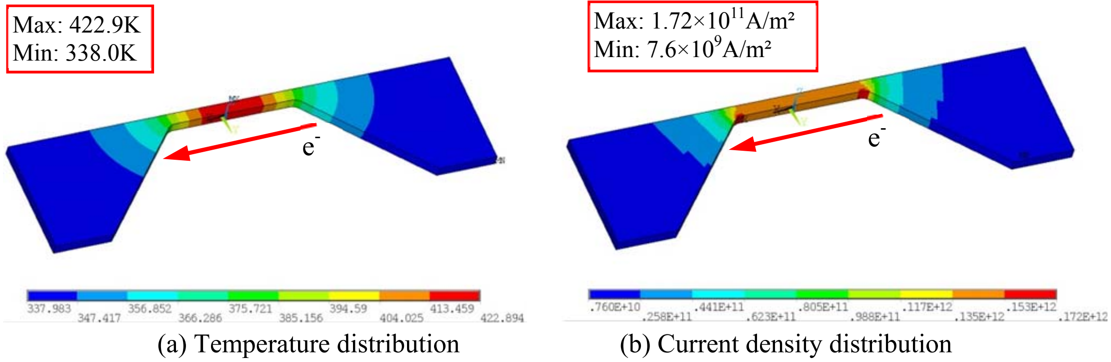

(a) Temperature distribution (b) Current density distribution

Figure 6. Temperature and current density distributions at initial time

Fig. 6 shows the temperature distribution and current density distribution under 1.48×10^{11}A/m² current density at initial time. Due to Joule heat, the maximum temperature occurs in the middle segment of the Al line. Therefore, the atom diffuses rapidly in the middle segment where it is easily induce void.

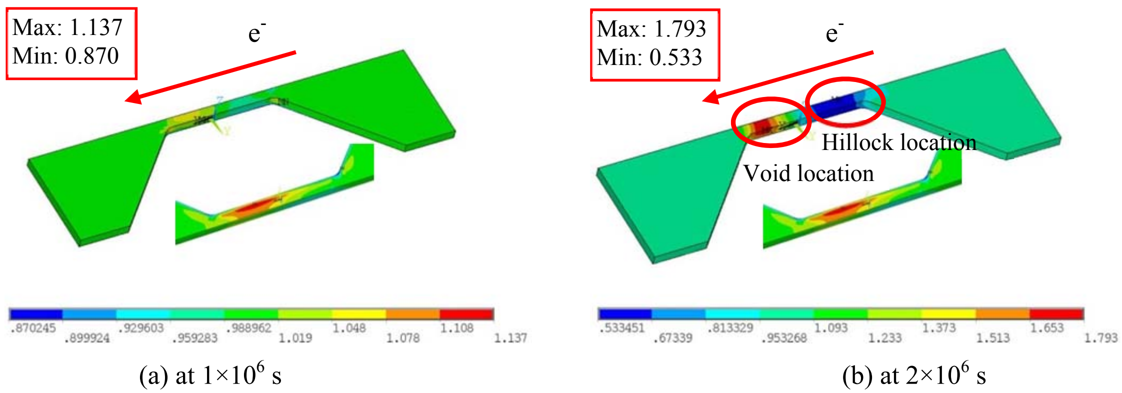

(a) at 1×10^6 s (b) at 2×10^6 s

Figure 7. NAD distribution after different time

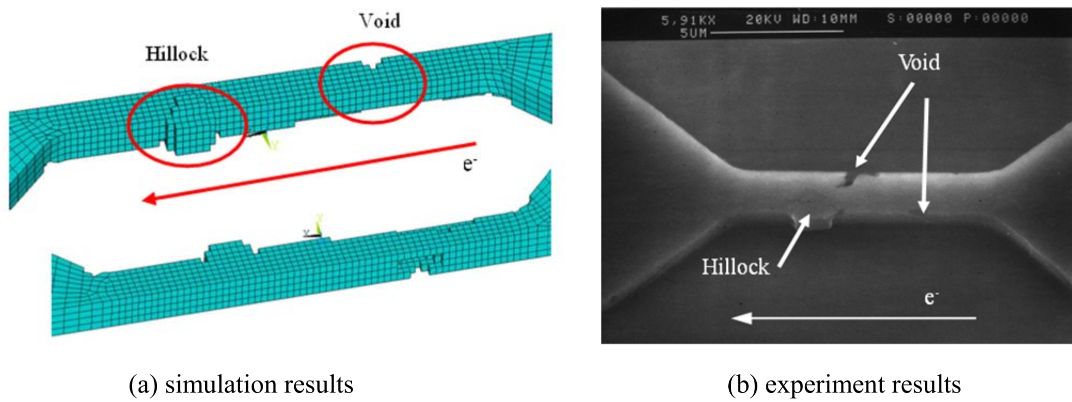

(a) simulation results (b) experiment results

Figure 8. Simulation and experiment results of void/hillock formation

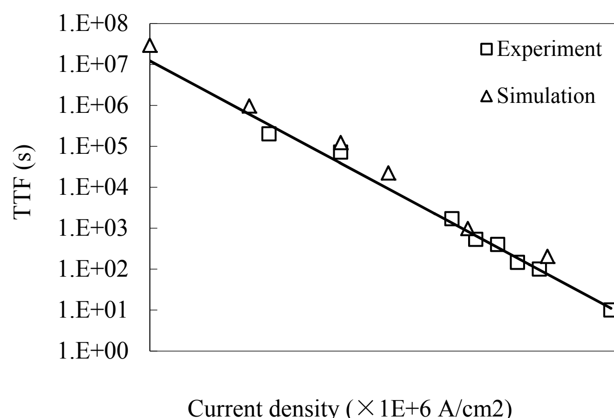

Figure 9. Comparison of the simulation results for TTF and the experimental test results

Assume no EM void produces in the analysis (static analysis). Fig. 7 shows the NAD distribution of the SWEAT structure after different time, the zone with minimum normalized atomic density has expanded to the whole quarter segment of Al metallization from left. These may be due to the hydrostatics stress that dominates the EM diffusion at the begin time, while with the increment of the time, current density and atomic density gradient dominate the EM diffusion gradually. Furthermore, according to the normalized atomic density distribution, the void and hillock formation can be simulated, seen as in Fig. 8(a). The result is consistent with the picture observed in the experiment [13], as shown in Fig. 8(b).

A comparison of the simulation results for TTF and the previous experimental test results obtained in ref. [13] is also presented in Fig. 9. It can be founded that the simulated TTF life data agrees well with the experimental data.

6. Conclusions

The numerical simulation method for electro-migration induced void and hillock evolution in IC interconnect structures is studied in this paper. The methodology is developed based on the discretized weighted residual method to solve the local EM mass continuity equation with the variable of atomic density. Since it takes the advantage of solving the variable of atomic density, it avoids directly solving the divergences of the atomic flux, which includes the atomic density gradient items and is very hard and challenging to get the solution by traditional method. This method has been implemented in the commercial software ANSYS Multiphasic in combined with a user defined FORTRAN code that computes the atomic density redistribution. The simulation and comparison with the measured results in interconnects of a SWEAT structure are presented and discussed. The results show that the investigation method developed in this paper has demonstrated reasonable predicted result for void and hillock in electro-migration failure.

References

[1] Croes, Kristof, et al. "Interconnect reliability–A study of the effect of dimensional and porosity scaling." Microelectronic Engineering 88.5 (2011): 614-619.

[2] Black, James R. "Mass transport of aluminum by momentum exchange with conducting electrons." Reliability Physics Symposium, 1967. Sixth Annual. IEEE, 1967.

[3] Tu, K. N. "Recent advances on electromigration in very-large-scale-integration of interconnects." Journal of applied physics 94.9 (2003): 5451-5473.

[4] Liang, S. W., T. L. Shao, and Chih Chen. "3-D simulation on current density distribution in flip-chip solder joints with thick Cu UBM under current stressing." Electronic Components and Technology Conference, 2005. Proceedings. 55th. IEEE, 2005.

[5] Dalleau, D., and K. Weide-Zaage. "Three-dimensional voids simulation in chip metallization structures: a contribution to reliability evaluation." Microelectronics Reliability 41.9 (2001): 1625-1630.

[6] Basaran, Cemal, and Minghui Lin. "Damage mechanics of electromigration induced failure." Mechanics of Materials 40.1 (2008): 66-79.

[7] Sukharev, Valeriy, and Ehrenfried Zschech. "A model for electromigration-induced degradation mechanisms in dual-inlaid copper interconnects: effect of interface bonding strength." Journal of applied physics 96.11 (2004): 6337-6343.

[8] Stolarska, M., and D. L. Chopp. "Modeling thermal fatigue cracking in integrated circuits by level sets and the extended finite element method." International journal of engineering science 41.20 (2003): 2381-2410.

[9] Pak, J. S., et al. "Modeling of electromigration in through-silicon-via based 3D IC." Electronic Components and Technology Conference (ECTC), 2011 IEEE 61st. IEEE, 2011..

[10] Reddy, Junuthula Narasimha. An introduction to the finite element method. Vol. 2. No. 2.2. New York: McGraw-Hill, 1993.

[11] Sasagawa, Kazuhiko, et al. "Prediction of electromigration failure in passivated polycrystalline line." Journal of Applied Physics 91.11 (2002): 9005-9014.

[12] Clement, J. J. "Vacancy supersaturation model for electromigration failure under dc and pulsed dc stress." Journal of applied physics 71.9 (1992): 4264-4268.

[13] Dalleau D. 3-D time-depending simulation of void formation in metallization structures. Doctor Dissertation, Hannover University, 2003.

[14] Yamagata, Yutaka, et al. "A micro mobile mechanism using thermal expansion and its theoretical analysis. A comparison with impact drive mechanism using piezoelectric elements." Micro Electro Mechanical Systems, 1994, MEMS'94, Proceedings, IEEE Workshop on. IEEE, 1994.